Torque Estimation Using Precise Calculations of Inductance and Iron loss Mathematization

Gyu-Won Cho *, and Gyu-Tak Kim *

Abstract – **The torque was calculated with inductance and iron loss. Because the linkage flux can change the inductance, and q-axis current can change the iron loss. Therefore, precise estimation of torque can achieve with the inductance and iron loss detail calculations. So, in this paper, the d, q-axis inductance was verified through CVCT(Current Vector Control Test) and DCT(Direct Current Test). Also in the iron loss calculation, the prediction of all areas of current magnitude, phase angle and speed was very difficult. And LUT(Look-Up Table) was spent time and resource largely. Therefore, iron loss mathematization was proposed according to current magnitude, phase angle and speed. Also, characteristics of IPMSM were comprised of analyzed and experimental values.**

1. Introduction

Generally, operating characteristics of IPMSM (Interior Permanent Magnet Synchronous Motor) were estimated with d, q-axis equivalent circuit. If a calculation of non-linear parameters was exactly performed, it is known as a efficient method [1]-[2].

However, the inductance values of the d, q-axis vary nonlinearly under different operating conditions because the magnitude and phase angle of the input current can change the magnetic flux distributions, and the saturation of magnetic materials in the motor can change the machine reluctance [3]. Therefore, estimation of the detailed d, q-axis inductance is very important.

Non-linear parameters were applied to LUT (Look-Up Table), because non-linear parameters calculation was relatively difficult and delicate. But, the iron loss was largely changed according to current magnitude, phase angle and speed by iron core's magnetic field variation [4]. Also, usually, the iron loss resistances were calculated at particular input state, and those results were applied to an equivalent circuit by LUT. And, estimation of operating characteristics by field-weakening control, voltage and current limits was very complicated parameters. And, LUT took lots of time and resource.

Therefore, in this paper, the inductance was calculated through a CVCT and DCT and the results were compared and studied. Also, the iron loss mathematization was

proposed according to current magnitude, phase angle and speed. Because, the iron loss should respond very quickly to variation of input parameters. Also, characteristics of IPMSM were comprised of analyzed and experimental values.

2. Estimation of d, q-axis Inductance

Table 1 shows the motor specification. The d, q-axis inductance was calculated by the voltage equation and vector diagram of IPMSM from formula [5]. So, numerical formula of inductance was described as the d, q-axis current variation according to linkage flux change.

Table 1. Specification of model

Item	Specification
Rated Speed (rpm)	3000
Rated Torque (Nm)	1.85
Pole/Slot	8/12
Air-gap Length (mm)	1
Winding Type	Concentrated winding
Br (T)	1.3
Stack Length (mm)	45
Stator Diameter (mm)	83.6
Phase resistance(ohm)@75˚C	0.0235

Fig. 1 shows a linkage flux change according to current phase angle. The d-axis current was increased by the increased current phase angle. And, total linkage flux was decreased, and phase gap became smaller, because q-axis

* Dept. of Electrical Engineering, Changwon National University, Korea.(gtkim@changwon.ac.kr)
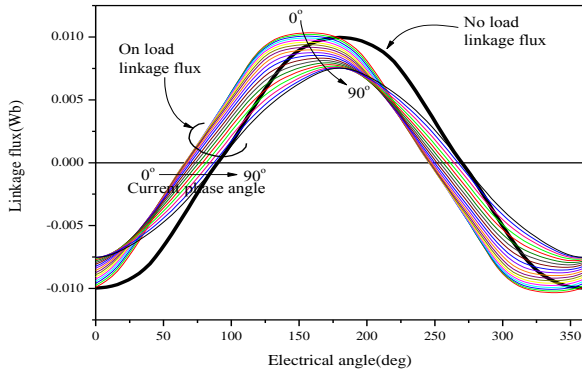
current was decreased.

Fig. 1. Linkage flux according to change of current phase angle

2.1 Current Vector Control Test (CVCT)

CVCT was not required for additional experimental equipment, except controller for operating [6]-[7]. That is a very major advantage. The inductance by CVCT was calculated through the measurement of back-EMF, the phase current and phase voltage as rotating. In addition, CVCT can calculate inductance according to the current magnitude and the current phase angle.

The flux of Permanent Magnet (PM) was calculated as constant value. Therefore, air-gap's magnetic flux density has sinusoidal waveform. Beside, the phase voltage and current was considered as only fundamental wave through Fast Fourier Transform (FFT).

The numerical formula of inductance can be obtained by voltage equation of (1), and (2).

$$\begin{bmatrix} v_d \\ v_q \end{bmatrix} = \begin{bmatrix} R_s + \rho L_d & -\omega L_q \\ \omega L_d & R_s + \rho L_q \end{bmatrix} \begin{bmatrix} i_d \\ i_q \end{bmatrix} + \begin{bmatrix} 0 \\ \omega \phi_a \end{bmatrix} \tag{1}$$

$$L_d = \frac{v_q - R_s i_q - \omega \phi_a}{\omega i_d}$$
$$L_q = \frac{-v_d + R_s i_d}{\omega i_q} \tag{2}$$

Fig. 2 shows the experimental equipment. Fig. 3 shows the result of CVCT. For the average error of the inductance, L_d was as much as 2.92% and L_q was 4.5%. The error is caused by the fundamental wave detection of PWM, location alignment of the encoder, temperature rise of the permanent magnet and etc.

2.2 Direct Current Test(DCT)

The DCT method fixes the rotor. Thereafter, the power supply was cut off after enough a flow of direct current. Then, the waveform, at which the current is reduced to 0, was measured. In this case, the iron loss is not included, which is advantageous. In addition, interference between the d, q-axis does not occur, because the direct current is applied. However, the current phase angle cannot be considered. Therefore, the device can be arrest at $i_d=0$ or $i_q=0$ positions. The formula of the inductance by stationary rotor is obtained by (3) ~ (6).
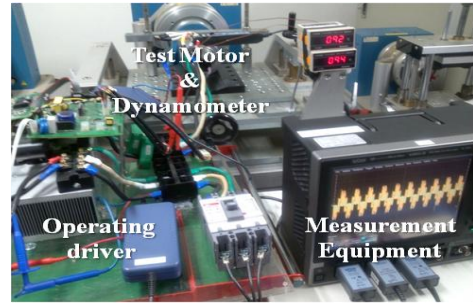

Fig. 2. The CVCT experimental equipment

$$\begin{bmatrix} v_d \\ v_q \end{bmatrix} = \begin{bmatrix} R_s + \rho L_d & -\omega L_q \\ \omega L_d & R_s + \rho L_q \end{bmatrix} \begin{bmatrix} i_d \\ i_q \end{bmatrix} \tag{3}$$

$$v_d = R_s i_d + \frac{d}{dt} L_d i_d \tag{4}$$

The switch of the power is open, the current starts to decrease and the voltage and current are changed as given in (5) according to time. $i_u(t)$ is the current change according to time and i_0 is the initial current value.

$$\int V_D(t)dt - \int R_s i_u(t)dt = L_d i_0 \int \frac{d}{dt} dt \tag{5}$$

$$L_d = \frac{\int \frac{2}{3} V_D(t)dt + \int R_s i_u(t)dt}{i_0}$$

$$L_q = \frac{\int \frac{2}{3} V_D(t)' dt + \int R_s i_u(t)' dt}{i_0'} \tag{6}$$

Fig. 4 shows DCT experimental equipment. Fig. 5 shows a comparison of the inductance by the DCT and the analys is values. In L_d, 6.4% error was generated and 0.8% was ge nerated in L_q. The magnetic flux's path of q-axis was simpler than that of d-axis, and the air-gap is located at the both sides of the axis center. Therefore, the lineup is very sensitive. It is hard to say that error was not generated in L_q. But, the PM was located at magnetic pa th of d-axis and, the lineup is very difficult. The error of d-axis was generated more than q-axis.
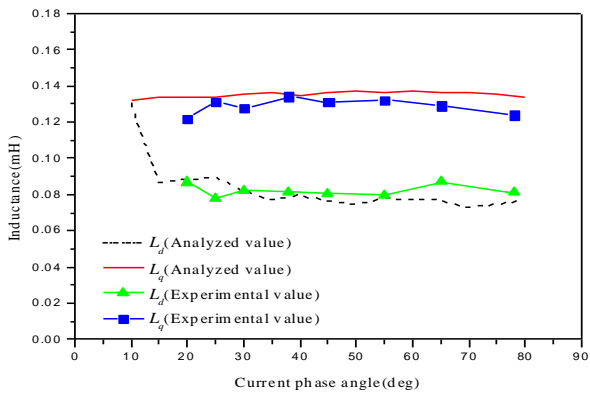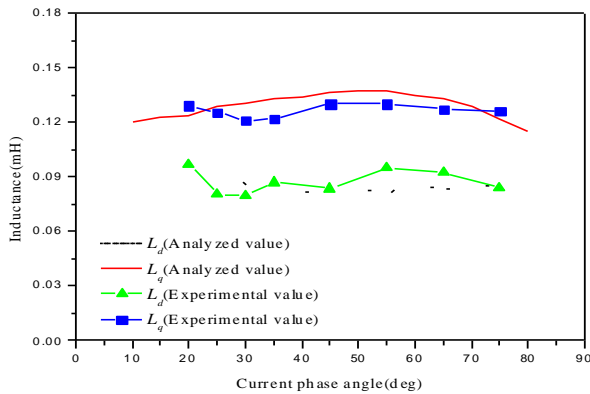
(a) 12(A)
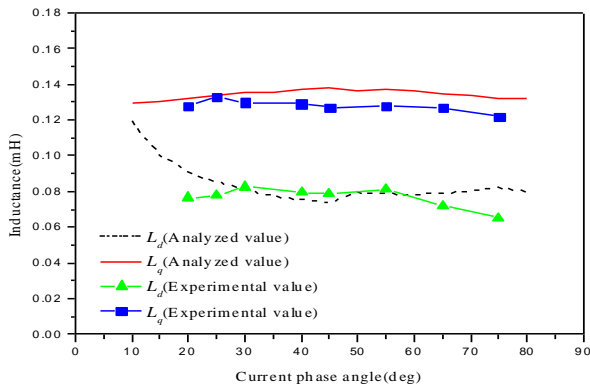
(b) 18(A)
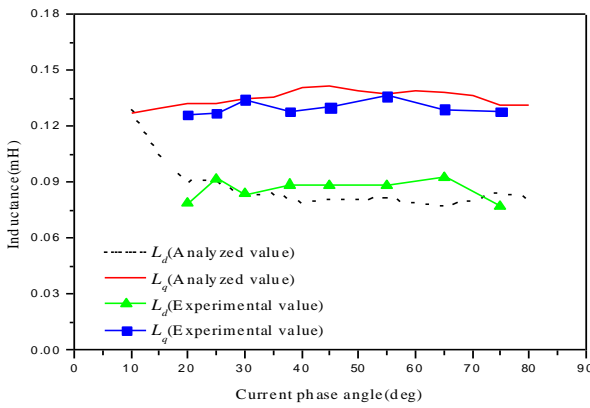
(c) 24(A)

(d) 30(A)
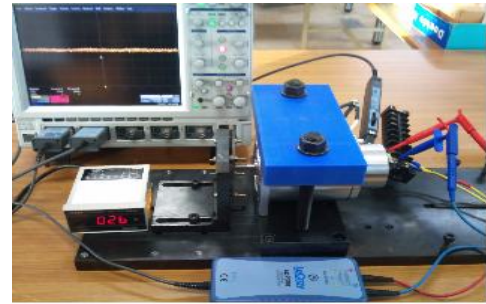**Fig. 3.** The result of CVCT and FEM

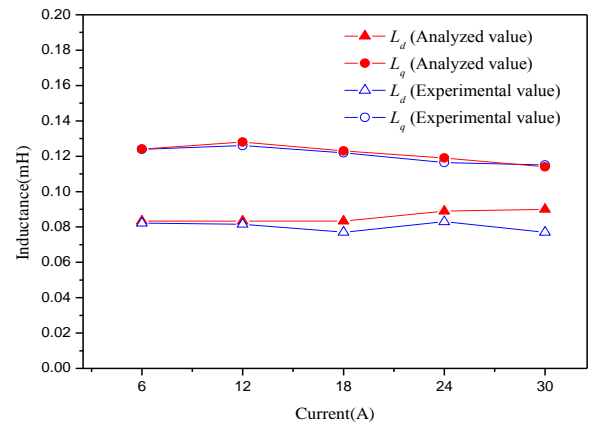**Fig. 4.** DCT experimental equipment

Fig. 5. DCT Comparison of result

Fig. 6 shows inductance profile according to the current. The inductance was made by using CVCT and DCT. The inductance's propriety was verified through torque experiment according to current.
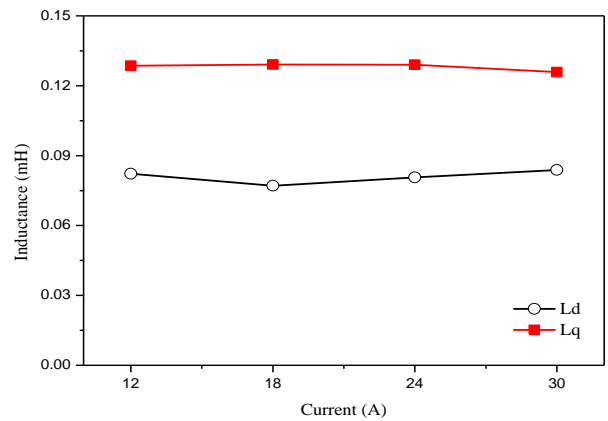

Fig. 6. The average of inductance according to current

3. The Iron Loss Mathematization

The iron loss equation has certain current magnitude, phase angle and speed conditions. Therefore, iron loss was changed by frequency according to operating speed by load condition and flux-density according to current phase angle

in the iron core. In that case, the iron loss should be evaluated repeatedly. Much time and resource were needed with this calculation method. Especially, IPMSM has the widely operating speed area like a field-weakening control, so disadvantages must be overcome in IPMSM.

Fig. 7 shows the iron loss mathematization progress. The iron loss equation was transformed with a formula of speed. And then, the iron loss mathematization according to current phase angle was performed. Finally, the iron loss was recalculated by formula of current magnitude.
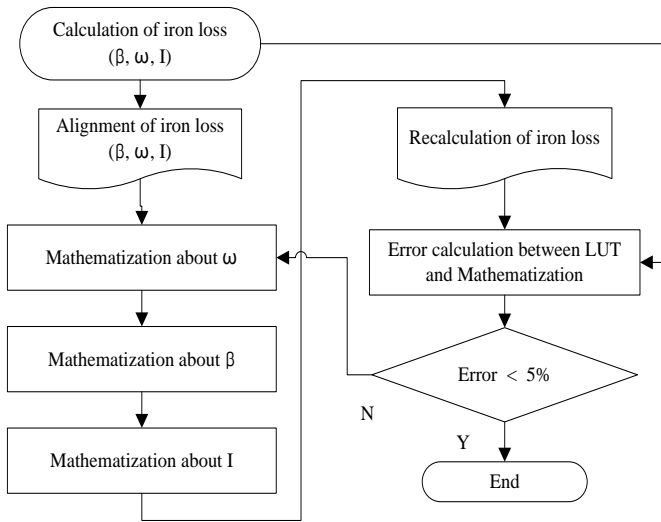

Fig. 7. Flow chat of iron loss mathematization

Fig. 8 shows the iron loss variation according to speed, current magnitude and phase angle.

The formula according to the current phase angle, speed can be obtained by (7).

Here, N_s is the operating speed, β is the current phase angle, I is current, $z_0 \sim z_2$ are intercept of each equation, $A_1 \sim A_6$ are mathematization coefficients. So, the iron loss was transformed with the equation according to speed, current magnitude and phase angle. Consequentially, the iron loss was very simply calculated from input parameters such as speed, current and current phase angle. It was very powerfully advantage on the calculation of operating characteristics.

$$W_i = \{z_0 + (A_1 \cdot \beta) + (A_2 \cdot \beta^2)\} + \{(z_1 + (A_3 \cdot \beta) + (A_4 \cdot \beta^2)\}N_s + \{(z_2 + (A_5 \cdot \beta) + (A_6 \cdot \beta^2)\}N_s^2$$

(7)

where, $z_0 = a + (b \cdot I)$,

$z_1, z_2, A_1, A_2, A_3, A_4, A_5, A_6 = a + (b \cdot I) + (c \cdot I^2)$

Fig. 9 shows the comparison of LUT and mathematization of the iron loss. The error was generated

under 1%. The output characteristic experiment was performed by measurement of output power and input power.

Fig. 10 shows variation of total torque. When the maximum torque generation, the torque was 1.87(Nm) at current phase angle 10°. It result was recalculated from 1.92(Nm) of torque without iron loss. Because, q-axis current was decreased by an iron loss current.
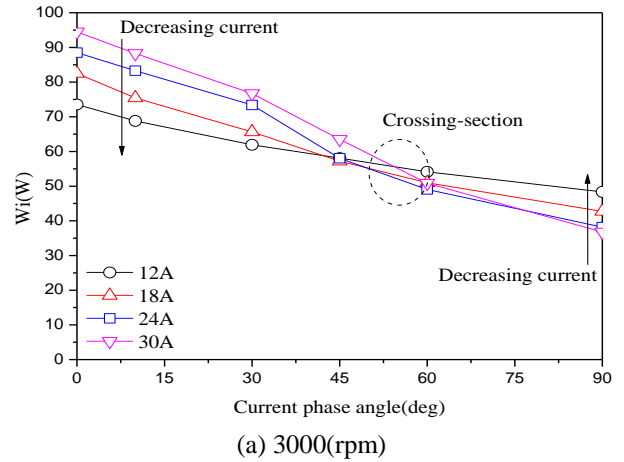
(a) 3000(rpm)
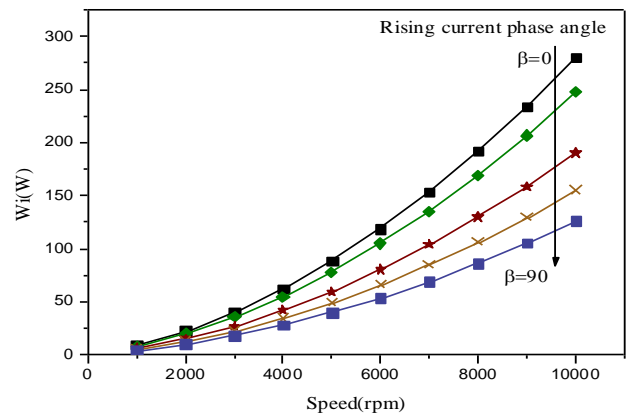
(b) 24(A)

Fig. 8. Iron loss variation according to speed each current

4. Experimental Results

The inductance is a parameter that directly affects the torque in d, q-axis equivalent circuit. Also, the iron loss affects q-axis current, so the torque changes with the iron loss. Therefore, precise calculation of torque compared with the experiments is very important. In this paper, at rated current and speed, the torque was measured according to current phase angle, and it was compared with experimental result.

Fig. 11 shows the torque experimental equipment, and Fig. 12 shows measured waveforms of voltage, current and

encoder pulse.

The torque experimental results are shown in Fig. 13. From the results, the maximum torque was generated at a current phase angle of 10°. As a result, the torque calculation using precise inductance and iron loss does not include the error almost.
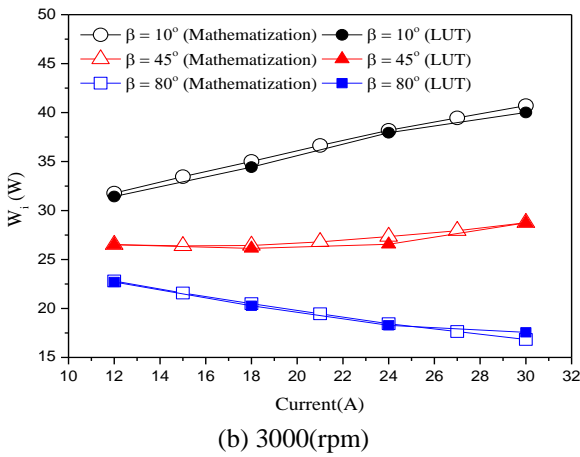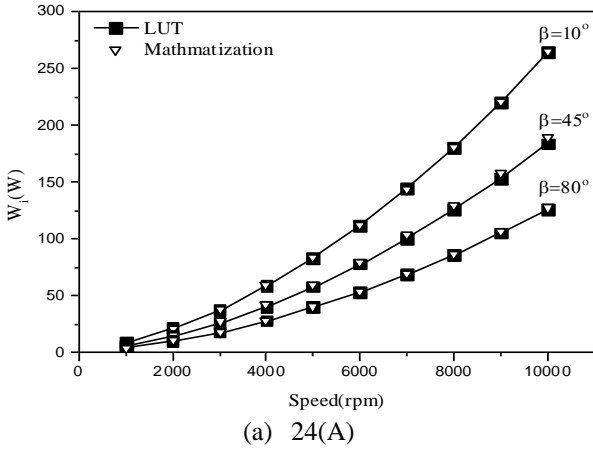

(a) 24(A)

(b) 3000(rpm)
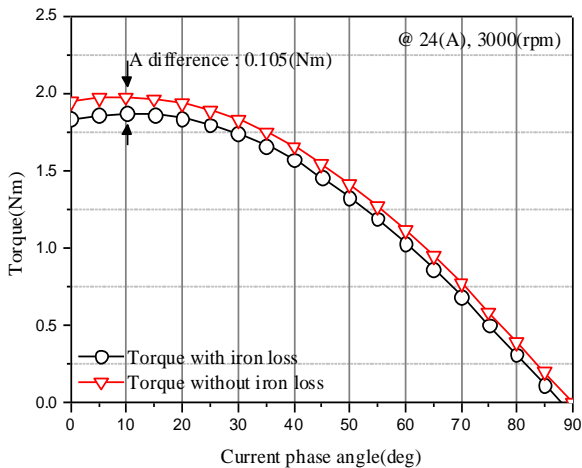
Fig. 9. Comparison of LUT and mathematization results
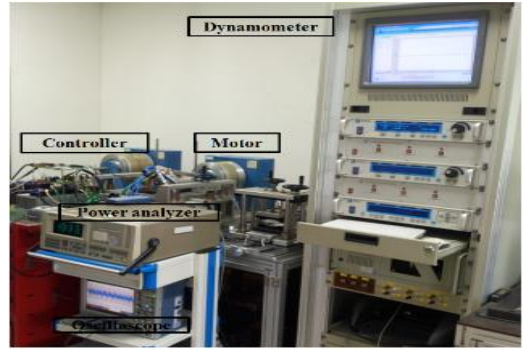

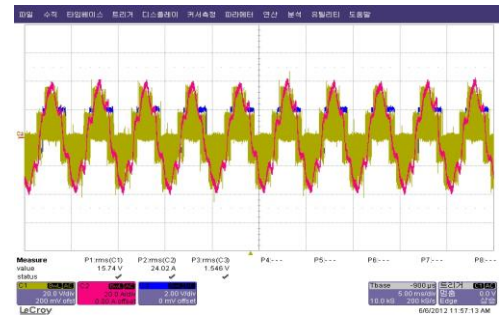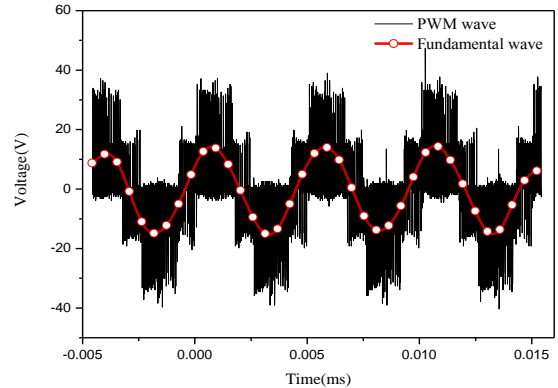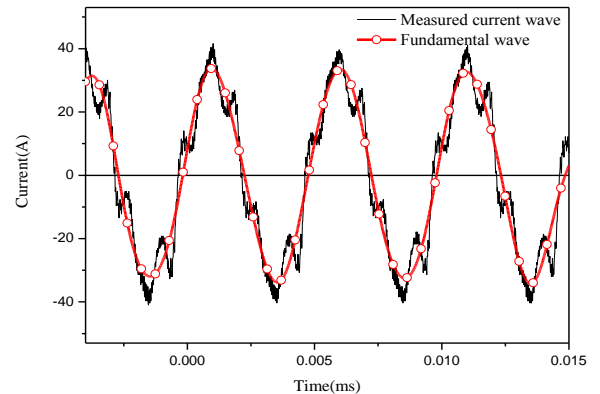**Fig. 10.** Generated torque in consider of iron loss

Fig. 11. Experimental equipments

(a) Measured pulses

(b) Fundamental waveform of voltage

(c) Fundamental waveform of current

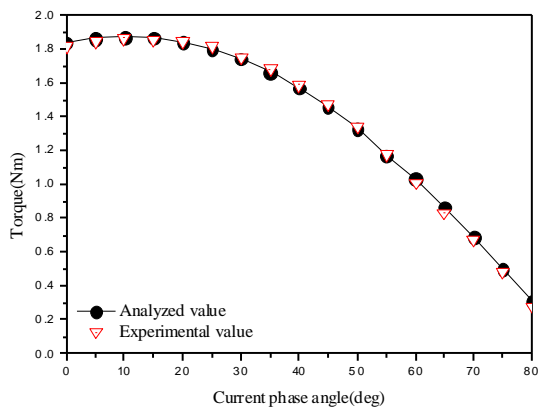**Fig. 12.** Measured waveforms of voltage, current and encoder pulse

Fig. 13. Experimental results

5. Conclusion

In this paper, the torque was estimated by inductance and iron loss. So, inductance of IPMSM was precisely calculated by CVCT and DCT. The average value of inductance was computed by supplement of strengths and weaknesses about CVCT and DCT. And the adequacy of inductance calculation was verified by comparison of experiment with calculation of torque. And the iron loss was transformed for simply calculation in variation operating condition.

The inductance and iron loss directly affect the torque calculation. So, calculations of inductance and iron loss were performed for precise torque estimation. The motor of vehicle has characteristics of low turn and largely diameter of conductor due to low voltage and high current. Therefore, a measurement error and a calculation error were constrainedly generated due to very tiny inductance. But in this paper, the inductance by current magnitude and current phase angle was calculated by two experimental methods. So, analyzed and experimental value was almost same, and satisfactory results were obtained.

Acknowledgements

References

[1] J.-W. Jung, J.-J. Lee, S.-O. Kwon, J.-P. Hong, and K.-N. Kim, "Equivalent circuit analysis of interior permanent magnet synchronous motor considering magnetic saturation", *IEEE Trans on Magnetics*, vol. 42, no. 4, pp.1303-1306, 2006.

[2] T. J. E. Miller, M. Popescu, C. Cossar, and M. Mc Gilp, "Performance Estimation of Interior Permanent-Magnet Brushless Motors Using the Voltage-Driven Flux-MMF Diagram," *IEEE Trans On Magnetics*, vol. 42, no. 7, pp. 1867~1872, 2006.

[3] L. Chedot and G. Friedrich, "A Cross Saturation Model for Interior Permanent Magnet Synchronous Machine. Application to a Starter-Generator," *IEEE Industry Application Conference,* vol. 1, pp. 64~70, 2004.

[4] D. M. Ionel, M. Popescu, S. J. Dellinger, T. J. E.Miller, R. J. Heideman, and M. I. McGilp, "On the variation with flux and frequency of the coreloss coefficients in electrical machines," *IEEE Trans on Industry Applications*, vol. 42, no. 3, pp. 658–668, 2006.

[5] S. Morimoto, M. Sanada and Y. Taketa, "Wide-Speed Operation of interior Permanent Magnet Synchronous Motors with High-Performance Current Regulator,*" IEEE Trans. Industry Applications*, vol. IA-30, no. 4, July/Aug., pp. 920~926, 1994.

[6] Vernon. B, Honsinger, "The Inductance Ld and Lq of Reluctance Machines", *IEEE Trans. On Power Apparatus and Systems*, vol. pas-90, no. 1, 1971.

[7] Morimoto. S, Takeda. Y, Hirasa. T, Taniguchi. K, "Expansion of Operating Limits for Permanent Magnet Motor by Current Vector Control Considering Inverter Capacity", *IEEE Trans. On Industry Application*, vol.26, no. 5, pp. 866~871, 1990.

Gyu-Won Cho received B.S and M.S degree in electrical engineering from Changwon National University, Korea. He is currently pursuing his Ph.D. degree at Changwon National University. His research interests are electrical machine and FEM analysis.

Gyu-Tak Kim received B.S, M.S and Ph.D degree in electrical engineering from Hanyang University, Korea. He is presently a Professor of Changwon National University. His research interests are electrical machine and FEM analysis.